European Journal of Medicinal Chemistry 44 (2009) 3280–3284

Contents lists available at ScienceDirect

European Journal of Medicinal Chemistry

journal homepage: http://www.elsevier.com/locate/ejmech

Short communication

Structure-based virtual screening approach to identify novel classes of PTP1B inhibitors

Hwangseo Park [a], Bharat Raj Bhattarai [b], Seung Wook Ham [c,*], Hyeongjin Cho [b,**]

[a] Department of Bioscience and Biotechnology, Sejong University, Seoul 143-747, Republic of Korea
[b] Department of Chemistry and Institute of Molecular Cell Biology, Inha University, 253 Yonghyun-dong, Nam-ku, Incheon 402-751, Republic of Korea
[c] Department of Chemistry, Chung Ang University, Seoul 156-756, Republic of Korea

ARTICLE INFO

Article history:
Received 8 September 2008
Received in revised form
2 February 2009
Accepted 12 February 2009
Available online 20 February 2009

Keywords:
Protein tyrosine phosphatase 1B, PTP1B
Structure–activity relationship
Virtual screening

ABSTRACT

Discovery of protein tyrosine phosphatase 1B (PTP1B) inhibitors has been actively pursued with the aim to develop therapeutics for the treatment of type 2 diabetes and obesity. We have been able to identify 9 novel PTP1B inhibitors by means of a computer-aided drug design protocol involving virtual screening with docking simulations under consideration of the effects of ligand solvation in the binding free energy function. Because the newly discovered inhibitors are structurally diverse and reveal a significant potency with IC_{50} values lower than 50 μM, all of them can be considered for further development by structure–activity relationship studies. Structural features relevant to the interactions of the newly identified inhibitors with the active-site residues of PTP1B are discussed in detail.

1. Introduction

Protein tyrosine phosphatase (PTP) was identified 2 decades ago by the purification of PTP1B from human placenta [1]. Subsequent human genome sequencing revealed the presence of more than 100 human PTPs [2]. As can be envisaged by the importance of PTPs in the cellular function, many of the PTPs are implicated in a variety of human diseases including diabetes, obesity, autoimmune diseases, infectious diseases, inflammation, cancer, osteoporosis, and neurodegeneration [3–5]. Among them, PTP1B is known to be associated with type 2 diabetes and obesity [6]. As an enzyme dephosphorylating the insulin receptor (IR) in skeletal muscle and liver, and Jak2 in hypothalamus, PTP1B regulates IR and leptin signaling, eventually acting as an important mediator for control of blood glucose levels and body weight [7–10]. When the PTP1B gene was disrupted or its expression suppressed in mice, reduced blood glucose levels and improved insulin responsiveness were observed in normal and diabetic mice [11–13]. PTP1B inhibition or a reduction of its cellular abundance in mice resulted in increased sensitivities to leptin and insulin, and has also exhibited a protective effect against diet-induced obesity [11,12,14]. On the basis of these observations, the inhibition of PTP1B has emerged as an attractive therapeutic strategy to treat type 2 diabetes and obesity, which has in the last decade motivated research in this field.

As recently reviewed in a comprehensive fashion [15,16], a large number of PTP1B inhibitors have been developed over the last decade in an effort to design potent and selective compounds as drug candidates. In the design of PTP inhibitors, the primary concern is the construction of a chemical structure that can mimic the phosphotyrosyl functional group to tightly bind in the highly conserved and polarized active site of PTPases. The previously used pTyr mimetics include methylenephosphonate, malonate, sulfate, carboxylate, and difluoromethylenephosphonate groups. Unfortunately, most of these multiple-charged phosphate-mimicking components have proven difficult to develop into effective drugs due to their low cell permeability and bioavailability. Therefore, new potential drug candidates targeting PTP1B need to be developed. Very recently, a selective noncompetitive PTP1B inhibitor, trodusquemine, developed by Genaera, proceeded to phase I clinical trials with promising preclinical and early clinical results as both an appetite suppressant and a hypoglycemic and hypocholestrolemic agent.

In the present study, we identified novel classes of PTP1B inhibitors by means of a structure-based drug design protocol involving virtual screening with docking simulations and an *in vitro* enzyme assay. The characteristic feature that discriminates our

Abbreviations: PTP, protein tyrosine phosphatase; IR, insulin receptor; *p*NPP, *p*-nitrophenyl phosphate; SAR, structure–activity relationship.

* Corresponding author. Tel.: +82 2 820 5203; fax: +82 2 825 4736.
** Corresponding author. Tel.: +82 32 860 7683; fax: +82 32 867 5604.
E-mail addresses: swham@cau.ac.kr (S.W. Ham), hcho@inha.ac.kr (H. Cho).

0223-5234/$ – see front matter © 2009 Elsevier Masson SAS. All rights reserved.
doi:10.1016/j.ejmech.2009.02.011

virtual screening approach from the others lies in the implementation of an accurate solvation model in calculating the binding free energy between PTP1B and putative ligands, which would have an effect of increasing the hit rate in the enzyme assay [17,18]. It will be shown that the docking simulation with the improved binding free energy function can be a useful tool for elucidating the activities of the identified inhibitors, as well as for enriching the chemical library with molecules that are likely to have desired biological activities.

2. Materials and methods

2.1. Materials

The docking library for PTP1B comprising about 85,000 compounds was constructed from the latest version of the chemical database distributed by Interbioscreen (http://www.ibscreen.com) containing approximately 30,000 natural and 320,000 synthetic compounds. Chemicals for the enzyme assay were purchased from Sigma (St. Louis, U.S.A.). A substrate, *p*-nitrophenyl phosphate (*p*NPP), for the PTP assay was obtained from Sigma in the di(Tris) salt form. The native form of PTP1B was expressed in an *Escherichia coli* expression system, and purified as described previously [19]. Absorbances were measured using Novaspec-II spectrophotometer (Amersham Pharmacia) or DU 650 spectrophotometer (Beckman Coulter).

2.2. Virtual screening of PTP1B inhibitors

The 3-D coordinates in the X-ray crystal structure of PTP1B complexed with an *N*-phenyloxamate inhibitor (PDB code: 1Q1M) [20] were selected as the receptor model in the virtual screening with docking simulations. After removing the ligand and solvent molecules, hydrogen atoms were added to each protein atom. Special attention was paid to assign the protonation states of the ionizable Asp, Glu, His, and Lys residues in the X-ray structure of PTP1B. The side chains of Asp and Glu residues were assumed to be neutral if one of their carboxylate oxygens pointed towards a hydrogen-bond accepting group including the backbone amino-carbonyl oxygen at a distance within 3.5 Å, a generally accepted distance limit for a hydrogen bond of moderate strength [21]. Similarly, the lysine side chains were assumed to be protonated unless the NZ atom was in proximity of a hydrogen-bond donating group. The same procedure was also applied to determine the protonation states of ND and NE atoms in His residues.

The compounds in the docking library were selected with the drug-like filters that select only the compounds with physico-chemical properties of potential drug candidates [22] and without reactive functional group(s). As a consequence of this filtering, the number of compounds decreases from 350,000 in the chemical database to 85,000 in the docking library. All of the compounds included in the docking library were then subjected to the Corina program to generate their 3-D atomic coordinates, followed by assignment of Gasteiger–Marsilli atomic charges [23]. We used the AutoDock program [24] in the virtual screening of PTP1B inhibitors because the outperformance of its scoring function over those of the others had been demonstrated in several target proteins [25]. AMBER force field parameters were assigned for calculating the van der Waals interactions and internal energy of a ligand as implemented in the AutoDock program. Docking simulations with AutoDock were then carried out in the active site of PTP1B to score and rank the compounds in the docking library according to their calculated binding affinities.

In the actual docking simulation of the compounds in the docking library, we used the empirical AutoDock scoring function improved by the implementation of a new solvation model for a compound. The modified scoring function has the following form:

$$\begin{aligned}\Delta G^{\mathrm{aq}}_{\mathrm{bind}} &= W_{\mathrm{vdW}} \sum_{i=1} \sum_{j>i} \left(\frac{A_{ij}}{r_{ij}^{12}} - \frac{B_{ij}}{r_{ij}^{6}} \right) + W_{\mathrm{hbond}} \sum_{i=1} \sum_{j>i} E(t) \\ &\quad \times \left(\frac{C_{ij}}{r_{ij}^{12}} - \frac{D_{ij}}{r_{ij}^{10}} \right) + W_{\mathrm{elec}} \sum_{i=1} \sum_{j>i} \frac{q_i q_j}{\varepsilon(r_{ij}) r_{ij}} + W_{\mathrm{tor}} N_{\mathrm{tor}} \\ &\quad + W_{\mathrm{sol}} \sum_{i=1} S_i \left(\mathrm{Occ}_i^{\max} - \sum_{j>i} V_j \mathrm{e}^{-(r_{ij}^2/2\sigma^2)} \right), \end{aligned} \tag{1}$$

where W_{vdW}, W_{hbond}, W_{elec}, W_{tor}, and W_{sol} are the weighting factors of van der Waals, hydrogen bond, electrostatic interactions, torsional term, and desolvation energy of inhibitors, respectively. r_{ij} represents the interatomic distance, and A_{ij}, B_{ij}, C_{ij}, and D_{ij} are related to the depths of the potential energy well and the equilibrium separations between the 2 atoms. The hydrogen bond term has an additional weighting factor, $E(t)$, representing the angle-dependent directionality. A cubic equation approach was applied to obtain the dielectric constant required in computing the interatomic electrostatic interactions between PTP1B and a ligand molecule [26]. In the entropic term, N_{tor} is the number of sp^3 bonds in the ligand. In desolvation terms, S_i and V_i are the solvation parameter and the fragmental volume of atom i [27], respectively, while $\mathrm{Occ}_i^{\max}$ stands for the maximum atomic occupancy. In the calculation of molecular solvation free energy term in Eq. (1), we used the atomic parameters recently developed by Kang et al. [28] because those of the atoms other than carbon were unavailable in the current version of AutoDock. This modification of the solvation free energy term is expected to increase the accuracy in virtual screening because the underestimation of ligand solvation often leads to the overestimation of the binding affinity of a ligand with many polar atoms [17].

The docking simulation of a compound in the docking library started with the calculation of the three-dimensional grids of interaction energy for all of the possible atom types present in chemical database. These uniquely defined potential grids for the receptor protein were then used in common for docking simulations of all compounds in the docking library. As the center of the common grids in the active site, we used the center of mass coordinates of the docked structure of the probe molecule, *N*-phenyloxamate, whose binding mode in the active site of PTP1B had been determined with X-ray crystallography and reported in PDB [20]. The calculated grid maps were of dimension $61 \times 61 \times 61$ points with the spacing of 0.375 Å, yielding a receptor model that includes the atoms within 22.9 Å of the grid center. For each compound in the library, 10 docking runs were performed with the initial population of 50 individuals. Maximum number of generations and energy evaluation were set to 27,000 and 2.5×10^5, respectively.

2.3. Enzymatic assay and IC_{50} determination

The compounds identified by virtual screening were tested for their ability to inhibit PTP1B, using *p*NPP as the substrate. The PTP1B activities were assayed in buffer A (100 mM Hepes, 5 mM EDTA, pH 7.0) at 37 °C in a final *p*NPP concentration of 2 mM. For the assay, the enzyme was diluted to a proper concentration with enzyme dilution buffer (25 mM Hepes, 5 mM EDTA, 1 mM DTT, and 1 mg/mL bovine serum albumin, pH 7.3). The concentration of PTP1B in the assay mixture was 2.1 μg/mL. A typical 50-μL reaction system contained 5 μL *p*NPP, 5 μL enzyme, 5 μL inhibitor dissolved in DMSO, 10 μL 5× buffer A, and 25 μL H_2O. After the mixture, without *p*NPP, had been incubated at 37 °C for 10 min, the enzyme

reaction was initiated by the addition of *p*NPP. After 3 min at 37 °C, the reaction was quenched by the addition of 0.5 M NaOH (0.95 mL), with the absorbance at 405 nm measured to quantify the *p*-nitrophenol produced. The IC_{50} values of the inhibitors were determined by measuring the *p*NPP hydrolase activity of PTP1B in a range of different inhibitor concentrations. The kinetic data were analyzed using the GraFit 5.0 program (Erithacus Software).

3. Results and discussion

Of the 85,000 compounds subject to the virtual screening with docking simulations, 250 top-scored compounds were selected as virtual hits. Among them, 248 compounds were available from the compound supplier and were evaluated for in vitro inhibitory activity against PTP1B. Twenty-three of the purchased compounds were excluded in the enzyme assay because of their low solubility both in water and in DMSO. As a result of the *in vitro* enzyme inhibition assay for the remaining 225 compounds, we identified 62 compounds that inhibited the catalytic activity of PTP1B by more than 50% at a concentration of 100 μM. Among them, 21 compounds revealed a significant potency with more than 90% inhibition at the same concentration and were selected to determine IC_{50} values. The known inhibitor, 2-(oxalyl-amino)-4,5,6,7-tetrahydro-thieno[2,3,*c*]pyridine-3-carboxylate (**10**, OATPC) was used as the reference in the enzyme inhibition assay because it had been identified as a competitive inhibitor of PTP1B in the previous study [29]. The chemical structures and the inhibitory activities of the newly identified inhibitors with IC_{50} values lower than 50 μM are shown in Fig. 1 and Table 1, respectively. Table 1 also lists the binding free energies of the inhibitors calculated during the virtual screening. We note that the known potent inhibitor Ertiprotafib gets a better score than most of the other inhibitors except for **2**, which compares well the corresponding IC_{50} values. It is also noteworthy that all of the newly identified inhibitors (**1**–**9**) exhibit a higher activity against PTP1B than the reference compound. To the best of our knowledge, none of the compounds shown in Fig. 1 have been reported as PTP1B inhibitors thus far. Furthermore, these newly found inhibitors are structurally diverse, and therefore each of which can be considered as a new inhibitor scaffold for further development by structure–activity relationship (SAR) studies or *de novo* design methods.

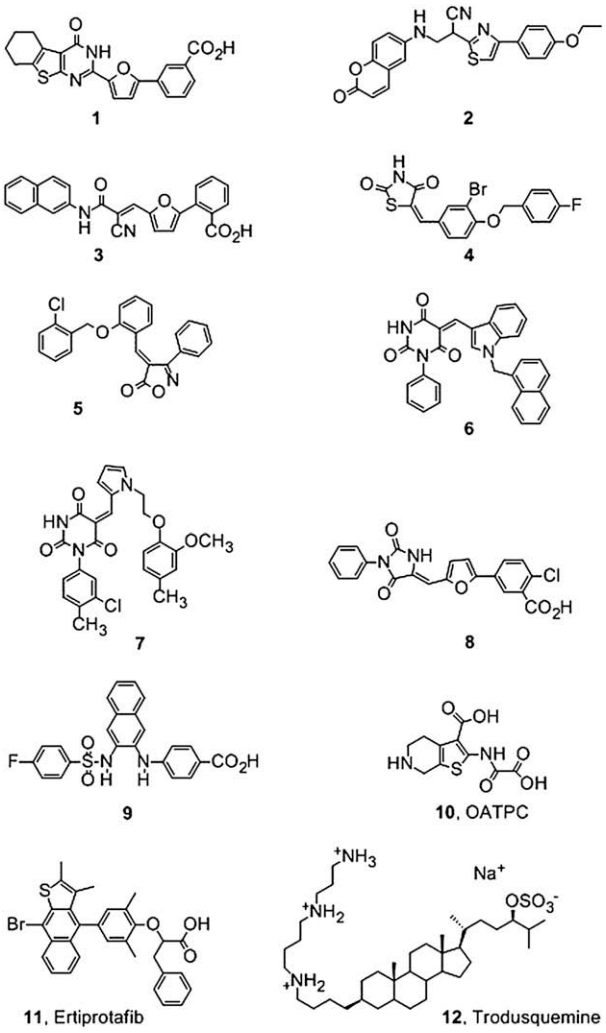

Fig. 1. Chemical structures of the newly identified PTP1B inhibitors (**1**–**9**) and compounds mentioned in this study (**10**–**12**).

Initial kinetic experiments with the identified compounds, **1**–**9**, revealed that **1** and **4** behaved as competitive inhibitors of PTP1B (data not shown). To obtain structural insight into the inhibitory mechanisms for the identified inhibitors of PTP1B, their binding modes in the active site were investigated using the AutoDock program in comparison with that of the known inhibitor OATPC. Fig. 2 shows the best-scored AutoDock conformations of OATPC, **4** and **1** in the active-site gorge of PTP1B. As revealed by the superposition of the docked structures, all of the inhibitors seem to be stabilized through interactions with 2 catalytic residues, Cys215 and Arg221, and the residues in the WPD loop. In order to examine the possibility of the allosteric inhibition of PTP1B by the inhibitors, docking simulations were carried out with the grid maps for the receptor model so as to include the entire portion of PTP1B. However, the binding configuration in which an inhibitor resides outside the active site was observed neither for the new inhibitors nor for OATPC. These results support the possibility that the inhibitors would impair catalytic activity of PTP1B through the specific binding in the active site.

The calculated binding mode of **4** in the active site of PTP1B is shown in Fig. 3. In the docking simulation, the amidic nitrogen of the thiazolidine-2,4-dione moiety was assumed to be deprotonated because the acidity of the thiazolidinedione proton had been found to be strong enough to permit its ionization constant ($pK_a \approx 6.74$) to be directly and accurately determined by conductivity measurements [30]. In the calculated PTP1B–**4** complex, we see that one of the aminocarbonyl oxygens of the inhibitor forms a bifurcated hydrogen bond with the side-chain guanidium group

Table 1
IC_{50} values (μM) of compounds **1**–**9** and reference compounds, **10** (OATPC) and Ertiprotafib, against PTP1B together with their calculated binding free energies during the virtual screening.

Compound	IC_{50}[a]	Binding free energy (kcal/mol)
1	25 ± 2	−23.67
2	28 ± 2	−24.18
3	27 ± 2	−23.01
4	11 ± 1	−23.72
5	22 ± 2	−22.56
6	12 ± 1	−23.05
7	35 ± 3	−23.39
8	34 ± 2	−23.18
9	41 ± 2	−22.41
10, OATPC	500 ± 100[b]	−22.03
Ertiprotafib	1.4 ± 0.1[b]	−23.83

[a] Values are the means ± standard deviations of 3 or more experiments. The kinetic data were analyzed using the GraFit 5.0 program (Erithacus Software).
[b] Data reproduced from our previous publication [19]. These data were obtained in an assay condition exactly the same as that for compounds **1**–**10**.

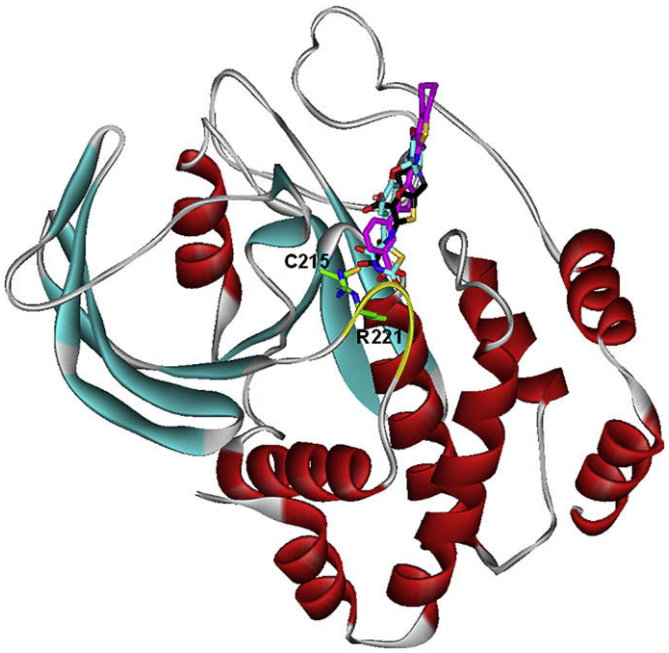

Fig. 2. Comparative view of the binding modes of the PTP1B inhibitors. Carbon atoms of the catalytic residues, OATPC, **4**, and **1** are indicated in green, black, cyan, and magenta, respectively. Indicated in yellow is the WPD loop.

of Arg221 and the backbone amidic nitrogen of Ser216. This hydrogen bond is apparently the strongest interaction in the enzyme–inhibitor complex, and expected to play a role of anchor for binding the inhibitor in the active site. The other aminocarbonyl carbon of **4** accepts an additional hydrogen bond in the active site from the side chain of Glu266. It is also noted that the deprotonated thiazolidine-2,4-dione moiety of **4** resides in the vicinity of the catalytic residue (Cys215) at a distance within 4–5 Å. The proximity to Cys215 with the hydrogen-bond stabilizations indicates that the deprotonated thiazolidinedione group may serve as an effective surrogate for the substrate phosphate group. Inhibitor **4** can be further stabilized in the active site by the hydrophobic interactions of its aromatic rings with the nonpolar residues including Tyr46, Val49, Phe182, and Ile218. On the basis of the structural features

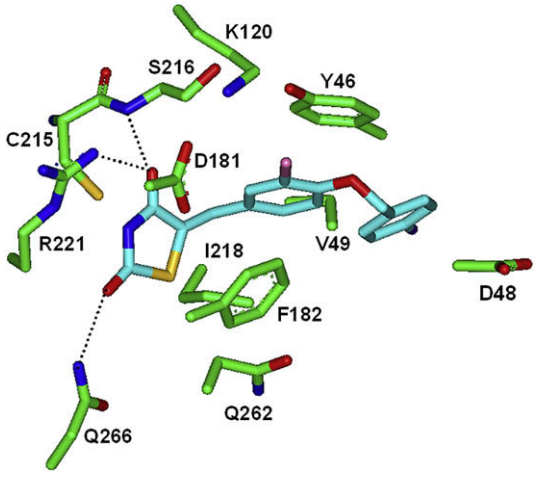

Fig. 3. Binding mode of compound **4** in the active site of PTP1B. Carbon atoms of the protein and the ligand are indicated in green and cyan, respectively. Each dotted line indicates a hydrogen bond.

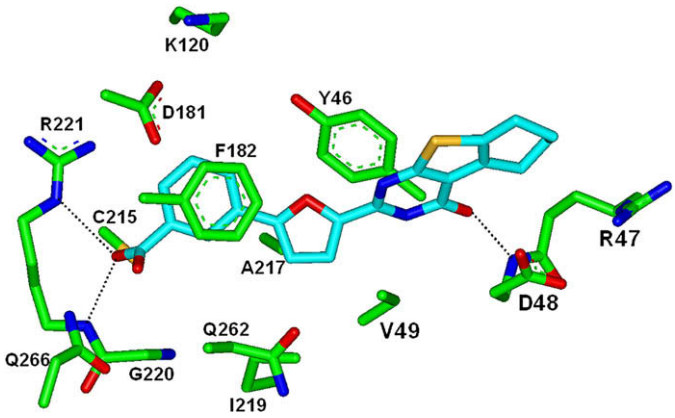

Fig. 4. Binding mode of compound **1** in the active site of PTP1B. Carbon atoms of the protein and the ligand are indicated in green and cyan, respectively. Each dotted line indicates a hydrogen bond.

derived from the calculated PTP1B–**4** complex, it can be argued that **4** should be capable of inhibiting the catalytic action of PTP1B by binding in the active site through the simultaneous establishment of the multiple hydrogen bonds and hydrophobic interactions.

Fig. 4 shows the lowest-energy binding mode of **1** in the active site of PTP1B. The role of a surrogate for the substrate phosphate group seems to be played by the benzoate moiety because it resides in the proximity of Cys215 with formation of the hydrogen bonds with protic residues in the active site. We note in this regard that one of the carboxylate oxygens receives 2 hydrogen bonds from the backbone amide group and the side-chain NE atom of Arg221. The binding mode of **1** differs from that of **4** in that a stable hydrogen bond is also established at the top of the active site between the aminocarbonyl group of **1** and the backbone amidic nitrogen of Asp48. As in the PTP1B–**4** complex, **1** forms van der Waals contacts with the side chains of Tyr46, Arg47, Val49, Phe182, Ala217, and Ile219, which should also be a significant binding force stabilizing **1** in the active site of PTP1B. Judging from the similarity in the hydrophobic interactions in PTP1B–**4** and PTP1B–**1** complexes, the decrease in the strength of hydrogen bonds with protic groups in the active site may be invoked to explain the 2-fold decrease in binding affinity in going from **4** to **1**.

In summary, we have identified 9 novel inhibitors of PTP1B by applying a computer-aided drug design protocol involving the structure-based virtual screening with docking simulations under consideration of the effects of ligand solvation in the scoring function. These inhibitors are structurally diverse and reveal a potency with IC_{50} values ranging from 10 to 50 μM. Therefore, each of the newly discovered inhibitors merits further development by structure–activity relationship studies or *de novo* design methods. Detailed binding mode analyses with docking simulation show that the inhibitors can be stabilized by the simultaneous establishment of multiple hydrogen bonds and van der Waals contacts in the active site.

Acknowledgments

B.R. Bhattarai was a recipient of a BK21 fellowship.

References

[1] N.K. Tonks, C.D. Diltz, E.H. Fischer, J. Biol. Chem. 263 (1988) 6722–6730.
[2] A. Alonso, J. Sasin, N. Bottini, I. Friedberg, A. Osterman, A. Godzik, T. Hunter, J. Dixon, T. Mustelin, Cell 117 (2004) 699–711.
[3] Z.-Y. Zhang, Curr. Opin. Chem. Biol. 5 (2001) 416–423.
[4] R.H. Van Huijsduijnen, A. Bombrun, D. Swinnen, Drug Discov. Today 7 (2002) 1013–1019.

[5] L. Li, J.E. Dixon, Semin. Immunol. 12 (2000) 75–84.
[6] Z.-Y. Zhang, S.-Y. Lee, Expert Opin. Investig. Drugs 12 (2003) 223–233.
[7] B.L. Seely, P.A. Staubs, D.R. Reichart, P. Berhanu, K.L. Milarski, A.R. Saltiel, J. Kusari, J.M. Olefsky, Diabetes 45 (1996) 1379–1385.
[8] J.M. Zabolotny, F.G. Haj, Y.B. Kim, H.J. Kim, G.I. Shulman, J.K. Kim, B.G. Neel, B.B. Kahn, J. Biol. Chem. 279 (2004) 24844–24851.
[9] W. Kaszubska, H.D. Falls, V.G. Schaefer, D. Haasch, L. Frost, P. Hessler, P.E. Kroeger, D.W. White, M.R. Jirousek, J.M. Trevillyan, Mol. Cell. Endocrinol. 195 (2002) 109–118.
[10] J.M. Zabolotny, K.K. Bence-Hanulec, A. Stricker-Krongard, F. Haj, Y.P. Wang, Y. Minokoshi, Y.-B. Kim, J.K. Elmquist, L.A. Tartaglia, B.B. Kahn, B.G. Neel, Dev. Cell 2 (2002) 489–495.
[11] M. Elchebly, P. Payette, E. Michaliszyn, W. Cromlish, S. Collins, A.L. Loy, D. Normandin, A. Cheng, J. Himms-Hagen, C.-C. Chan, C. Ramachandran, M.J. Gresser, M.L. Tremblay, B.P. Kennedy, Science 283 (1999) 1544–1548.
[12] L.D. Klaman, O. Boss, O.D. Peroni, J.K. Kim, J.L. Martino, J.M. Zabolotny, N. Moghal, M. Lubkin, Y.-B. Kim, A.-H. Sharpe, A. Stricker-Krongrad, G.I. Shulman, B.G. Neel, B.B. Kahn, Mol. Cell. Biol. 20 (2000) 5479–5489.
[13] B.A. Zinker, C.M. Rondinone, J.M. Trevillyan, R.J. Gum, J.E. Clampit, J.F. Waring, N. Xie, D. Wilcox, P. Jacobson, P. Frost, P.E. Kroeger, R.M. Reilly, S. Koterski, T.J. Opgenorth, R.G. Ulrich, S. Crosby, M. Butler, S.F. Murray, R.A. McKay, S. Bhanot, B.P. Monia, M.R. Jirousek, Proc. Natl. Acad. Sci. U.S.A. 99 (2002) 11357–11362.
[14] C.M. Rondinone, J.M. Trevillyan, J. Clampit, R.J. Gum, C. Berg, P. Kroeger, L. Frost, B.A. Zinker, R. Reilly, R. Ulrich, M. Butler, B.P. Monia, M.R. Jirousek, J.F. Waring, Diabetes 51 (2002) 2405–2411.
[15] S. Zhang, Z.-Y. Zhang, Drug Discov. Today 12 (2007) 373–381.
[16] S. Lee, Q. Wang, Med. Res. Rev. 27 (2007) 553–573.
[17] B.K. Shoichet, A.R. Leach, I.D. Kuntz, Proteins 34 (1999) 4–16.
[18] H. Park, Y.-J. Kim, J.-S. Hahn, Bioorg. Med. Chem. Lett. 17 (2007) 6345–6349.
[19] B.R. Bhattarai, S. Shrestha, S.W. Ham, K.R. Kim, H.G. Cheon, K.-H. Lee, H. Cho, Bioorg. Med. Chem. Lett. 17 (2007) 5357–5360.
[20] G. Liu, Z. Xin, Z. Pei, P.J. Hajduk, C. Abad-Zapatero, C.W. Hutchins, H. Zhao, T.H. Lubben, S.J. Ballaron, D.L. Haasch, W. Kaszubska, C.M. Rondinone, J.M. Trevillyan, M.R. Jirousek, J. Med. Chem. 46 (2003) 4232–4235.
[21] G.A. Jeffrey, An Introduction to Hydrogen Bonding, Oxford University Press, Oxford, 1997.
[22] C.A. Lipinski, F. Lombardo, B.W. Dominy, P.J. Feeney, Adv. Drug Deliv. Rev. 23 (1997) 3–25.
[23] J. Gasteiger, M. Marsili, Tetrahedron 36 (1980) 3219–3228.
[24] G.M. Morris, D.S. Goodsell, R.S. Halliday, R. Huey, W.E. Hart, R.K. Belew, A.J. Olson, J. Comput. Chem. 19 (1998) 1639–1662.
[25] H. Park, J. Lee, S. Lee, Proteins 65 (2006) 549–554.
[26] H. Park, J.H. Jeon, Phys. Rev. E 75 (2007) 021916.
[27] P.F.W. Stouten, C. Frömmel, H. Nakamura, C. Sander, Mol. Simul. 10 (1993) 97–120.
[28] H. Kang, H. Choi, H. Park, J. Chem. Inf. Model. 47 (2007) 509–514.
[29] H.S. Andersen, O.H. Olsen, L.F. Iversen, A.L.P. Sørensen, S.B. Mortensen, M.S. Christensen, S. Branner, T.K. Hansen, J.F. Lau, L. Jeppesen, E.J. Moran, J. Su, F. Bakir, L. Judge, M. Shahbaz, T. Collins, T. Vo, M.J. Newman, W.C. Ripka, N.P.H. Møller, J. Med. Chem. 45 (2002) 4443–4459.
[30] C.W. Kanolt, J. Am. Chem. Soc. 29 (1907) 1402–1416.